

MICROMECHANICAL "HOLLOW-DISK" RING RESONATORS

Sheng-Shian Li, Yu-Wei Lin, Yuan Xie, Zeying Ren, and Clark T.-C. Nguyen

Center for Wireless Integrated Micro Systems
Department of Electrical Engineering and Computer Science
University of Michigan, Ann Arbor, Michigan 48109-2122, USA

ABSTRACT

A vibrating polysilicon micromechanical "hollow-disk" ring resonator obtained by removing quadrants of material from a solid disk resonator, but purposely leaving intact beams of material to non-intrusively support the structure, has been demonstrated in several vibration modes spanning frequencies from HF (24.4 MHz), to VHF (72.1 MHz), to UHF (1.169 GHz), with Q 's as high as 67,519, 48,048, and 5,846, respectively. Furthermore, the use of notched support attachments closer to actual extensional ring nodal points raises the Q to 14,603 at 1.2 GHz, which is the highest yet achieved past 1 GHz, and which clearly illustrates the utility of notching for substantially higher Q . At 1.2 GHz, a combination of high Q and larger capacitive transducers allows the notched version to achieve an R_x of only 282 k Ω , which is 12X smaller than achieved by previous pure polysilicon surface-micromachined solid disk resonators in the GHz range.

1. INTRODUCTION

Wireless communication receivers could be greatly simplified if communication *channels* (rather than *bands* of channels) could be selected right at RF, immediately after the antenna, with out-of-channel noise and interferers removed before the received signal reaches any transistor circuits. With such an RF channel-selection capability, a wireless receiver might dispense with multi-stage down-conversion circuits, and instead, utilize a direct sub-sampling A/D converter right at the front end. Unfortunately, RF channel-selection is extremely difficult, because it requires at least 0.1% bandwidth selectivity, which in turn requires filters using resonators with Q 's $>10,000$ to maintain acceptable insertion loss (below 1 dB). Although on-chip MEMS-based vibrating resonators have very recently reached frequencies past 1 GHz [1], they have so far not done so with Q 's as high as 10,000. Even off-chip resonators in use today, such as SAW's or FBAR's, exhibit Q 's about an order of magnitude lower than the needed 10,000.

This work introduces a radial ring resonator that uses a centralized support structure and notching at the support attachment locations that together greatly reduce support losses and allow polysilicon ring resonator Q 's in excess of 10,000 at frequencies past 1 GHz. The specific design, shown in Fig. 1(a), is dubbed the "hollow-disk" ring resonator, since it is obtained by removing quadrants of material from a solid disk resonator [1], but purposely leaving intact beams of material to non-intrusively support the ring structure. Using an un-notched version of this design, several vibration modes have been demonstrated spanning frequencies from HF (24.4 MHz), to VHF (72.1 MHz), to UHF (1.169 GHz), with Q 's as high as 67,519, 48,048, and 5,846, respectively. With notched support attachments as depicted in Fig. 1(c), a Q of 14,603 has been achieved at 1.2 GHz, which represents the highest Q measured to date for

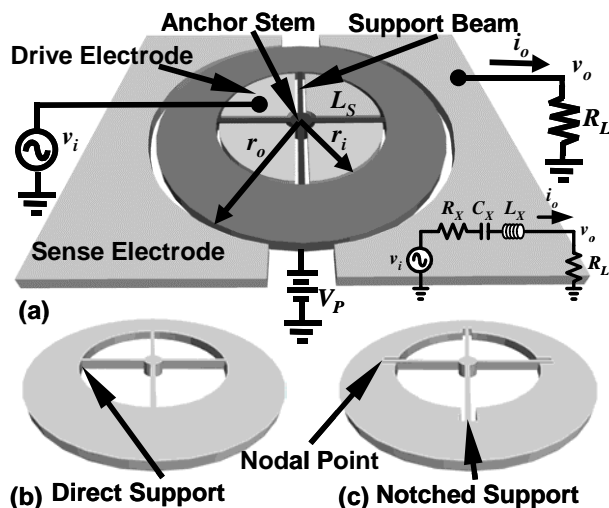


Fig. 1: (a) Perspective-view schematic of a micromechanical hollow-disk ring resonator in a typical two-port bias and excitation configuration with an equivalent LCR circuit model. (b) Direct support attachments. (c) Notched support attachments.

highest Q measured to date for any on-chip resonator past 1 GHz at room temperature, and which is now high enough to make possible RF channel-select filters with losses less than 1 dB. With electrodes both inside and outside the disk ring structure, this design attains electrode overlap advantages similar to that of a previously published annular ring design [2], while offering a much less intrusive support structure that not only enables substantially higher Q , but also enables impedances as low as 282 k Ω , which is 12X smaller than achieved by previous surface-micromachined, pure polysilicon, solid disk resonators operating past 1 GHz [1]. This paper details the design and fabrication principles that allow this hollow-disk ring to achieve frequencies and Q 's suitable for use in RF channel-select filters.

2. MAXIMIZING RESONATOR Q

One of the keys to attaining the exceptionally high Q at RF is in the non-intrusive suspension design, shown in Fig. 1(b). Here, the use of a centrally-located anchor with longitudinal-mode, quarter-wavelength, radial support beams provides a degree of balance and isolation that greatly suppresses anchor losses to the substrate, allowing this annular ring-type resonator to achieve Q 's much higher than versions where the ring is directly anchored to the substrate from underneath [2]. In particular, although locating anchors at nodal points—as done in [1][2] and some versions of [3]—does reduce energy transfer from a vibrating resonator to its anchors by virtue of the very little (ideally no) motion occur-

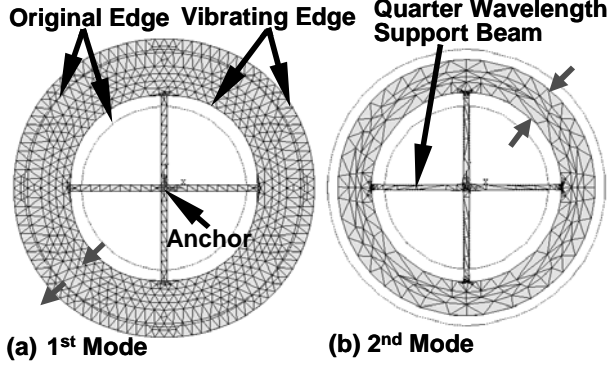


Fig. 2: Finite element simulated modes for the hollow-disk ring resonator of Fig. 1(b). (a) 1st contour mode (symmetric). (b) 2nd contour mode (anti-symmetric).

ring at the nodes, some energy is still lost since the anchors are inevitably finite in size, and thus, still attach to non-nodal (i.e., moving) locations immediately around the nodal *points*. If the resonator and anchor materials are identical, then direct attachment of the anchor (or stem) to the resonator constitutes a nearly perfect impedance match (i.e., a perfect energy transfer path) at the resonator-anchor interface [4], and this only exacerbates the loss issues. On the other hand, the use of quarter-wavelength support beam suspensions as shown in Fig. 1(b) effectively creates acoustic impedance-mismatches between the ring resonator and its distant anchors, which reflect wave energy back into the ring structure, minimizing energy losses, and maximizing the system Q .

The balanced suspension used in Fig. 1(b) offers the additional advantage of allowing symmetric, as well as anti-symmetric, contour modes, as shown in the ANSYS simulations of Fig. 2. The availability of both symmetric and anti-symmetric modes allows this device to invert the input-to-output phase difference of the resonator, which in turn facilitates the implementation of parallel filters [5] and mechanically-coupled arrays [6] for higher power handling ability and even lower impedance.

In addition to quarter-wavelength supports, the design of Fig. 1(c) goes one step further to reduce loss in the support structure of Fig. 1(b) by using notched ring attachment points that allow support beams to attach to the ring resonator structure closer to its actual nodal points. This further reduces acoustic losses through the support beams, allowing this annular ring-type resonator to achieve impressive Q 's in excess of 10,000 at UHF (as will be demonstrated shortly).

3. DEVICE OPERATION AND DESIGN

To excite this device in its two-port configuration (shown in Fig. 1(a)), a dc-bias voltage V_p is applied to the ring, and an ac signal v_i to its inner electrodes, generating an electrostatic force acting radially on the ring at the frequency of the ac input. When the frequency of v_i matches one of the ring's mode frequencies, the resulting force drives the ring into the corresponding vibration mode shape. For example, if the anti-symmetric mode of Fig. 2(b), the ring expands and contracts along its inner and outer perimeters. This motion creates a dc-biased (by V_p) time-varying capacitance between the ring and output electrode that then sources an output current i_o proportional to the amplitude of vibration. In effect, electrical input signals are converted to mechanical signals,

processed (with high Q) in the mechanical domain, then re-converted to electrical signals at the output, ready for further processing by subsequent transceiver stages. Electrically, this mechanical resonator device is equivalent to the LCR tank circuit shown in Fig. 1(a).

As indicated in Fig. 1(a), the vibrational resonance frequency is governed by the ring structure, which vibrates in contour mode shapes like those shown in Fig. 2. The use of a non-intrusive, centrally-anchored support in this device forces a sequenced design procedure, where the support structure must be designed first. The design sequence is such that the length of the radial support beams L_s is first set to correspond to one or more quarter-wavelengths at the desired resonance frequency f_o using the expression

$$L_s = \frac{n\sqrt{E/\rho}}{4f_o}, n=1,3,5... \quad (1)$$

where E and ρ are the Young's modulus and density, respectively, of the structural material, and n is the odd number of multiple quarter-wavelengths. The value of L_s then sets the inner radius of the ring r_i ; i.e., $r_i=L_s$. The outer radius r_o , can now be determined by solving the expression [7]

$$[J_1(hr_i)\sigma - J_1(hr_i) + r_i h J_0(hr_i)] \times [Y_1(hr_o)\sigma - Y_1(hr_o) + r_o h Y_0(hr_o)] - [Y_1(hr_i)\sigma - Y_1(hr_i) + r_i h Y_0(hr_i)] \times [J_1(hr_o)\sigma - J_1(hr_o) + r_o h J_0(hr_o)] = 0 \quad (2)$$

where L_s , r_i , and r_o are indicated in Fig. 1(a); σ is the Poisson ratio of the structural material; h is a frequency parameter; and J_0 (J_1), and Y_0 (Y_1) are Bessel functions of the first and second kinds, respectively. For a ring with $r_i=11.8 \mu\text{m}$ and $r_o=18.7 \mu\text{m}$, (2) yields a resonance frequency of 1.206 GHz.

It should be noted from (2) that the frequency of this device is independent of thickness to first order, so the designed frequency is relatively insensitive to process variations in thickness. As such, filters at many different frequencies, such as required by multi-band and RF channel-select applications, can be achieved in a single fabrication run, with one structural film deposition. This is a distinct advantage over most piezoelectric counterparts (e.g., FBARs, crystals) for which frequency is often determined primarily by thickness, making it difficult to manufacture several different multi-band frequencies on the same chip without the need for several structural film depositions, one for each frequency.

4. SERIES MOTIONAL RESISTANCE

The series motional resistance R_x is perhaps the most important of the elements in the equivalent circuit of Fig. 1(a), since it often governs the impedance matching and gain requirements for filters and oscillators, respectively, using this resonator. The R_x for the present device can be obtained by obtaining an expression for shunted output current i_o as a function of input drive voltage v_i using a procedure similar to that used in [8], then applying $R_x = v_i/i_o$. Doing so for the present device yields

$$R_x = \frac{v_i}{i_o} = \frac{k_r(r_i)}{j\omega_o \left(\frac{X(r_o)}{X(r_i)} \right) Q \eta(r_i) \eta(r_o)} \quad (3)$$

where $X(r)$ is the peak vibration displacement amplitude at radius r , ω_o is the angular resonance frequency, and where

$$\eta(r) = V_p \frac{\partial C}{\partial r} = V_p \frac{2\pi\epsilon_0 r H}{d_0^2} \quad (4)$$

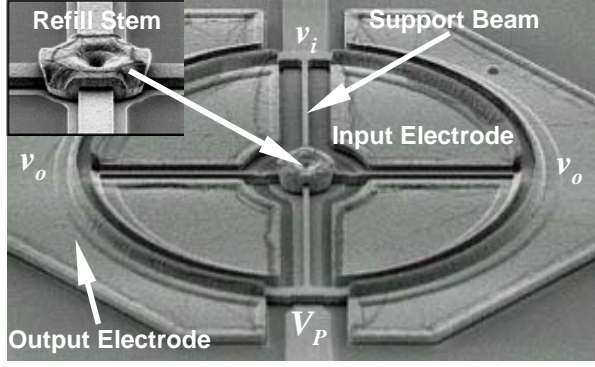


Fig. 3: Wide-view and stem-zoomed SEM's of a fabricated micromechanical hollow-disk ring resonator.

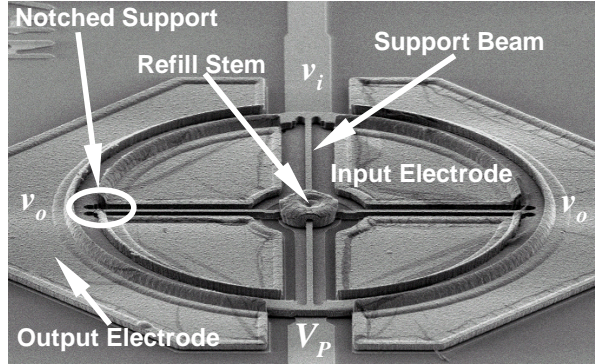


Fig. 4: A wide-view SEM of a fabricated notched micromechanical hollow-disk ring resonator.

Table 1: Series motional resistances R_x achievable by 3rd mode hollow-disk rings at 1.2 GHz with various characteristics. (a) Standard Case. (b) Large electrode overlap area. (c) Small gap spacing. (d) Large bias voltage. (e) Small Q .

Parameter	(a)	(b)	(c)	(d)	(e)	Units
r_i	11.8	146	11.8	11.8	11.8	μm
r_o	18.7	153	18.7	18.7	18.7	μm
d_o	100	100	50	100	100	nm
V_p	10	10	10	100	10	V
Q	15,000	15,000	15,000	15,000	1,000	--
R_x	274.4	27.1	17.1	2.7	4115.6	k Ω

$$k_r(r) = \omega_o^2 \frac{\int_{r_i}^{r_o} 2\pi r \rho H X^2(r) dr}{X^2(r)} \quad (5)$$

where ϵ_o is the permittivity in vacuum; r and H are the radius and thickness, respectively, of the ring; d_o is the electrode-to-resonator gap spacing; and V_p is the dc-bias voltage.

For a ring with $r_i=11.8 \mu\text{m}$, $r_o=18.7 \mu\text{m}$, $d_o=100 \text{ nm}$, $Q=15,000$, and a dc-bias voltage V_p of 10 V, (3) yields $R_x=274 \text{ k}\Omega$. Even lower values of R_x can be achieved with higher values of V_p . For example, a V_p of 100V would yield an R_x of 2.7 k Ω . Table 1 illustrates the wide range of series motional resistances R_x achievable by rings with various characteristics, illustrating the importance of structural radii r_i (r_o), gap spacing d_o , bias voltage V_p , and quality factor Q .

Of these " R_x -control parameters", the first based on scaling of the average ring radius is unique to ring resonator design, as previously pointed out in [2]. In particular, since the

frequency of a ring (given by (2)) is dependent mainly on its width ($r_o - r_i$), and relatively independent of its average radius, a ring is capable of achieving a specified frequency with any value of average radius. Thus, for any given frequency, the radius of a ring can be chosen as large as necessary to achieve an electrode-to-resonator overlap capacitance that yields a desired value of R_x . (In doing so, the support structure will need to set at multiple quarter-wavelengths, e.g., $3\lambda/4$, $5\lambda/4$, etc., in order to preserve anchor isolation.) The ability to do this is especially useful in applications where V_p is limited, or where the electrode-to-resonator gap spacing cannot be decreased, perhaps due to linearity constraints [9]. However, R_x reduction via radius scaling can be done only at the cost of die area. As illustrated by column (b) of Table 1, the ring radius must be increased by more than 10X to match the R_x reduction attained by a mere halving in electrode-to-resonator gap spacing. In this respect, radius scaling of single rings may not be as effective for R_x reduction as summing up the outputs of numerous smaller rings or solid disks, where even larger capacitive overlap areas should be achievable in the same amount of die area, and where signal-to-noise advantages also come into play, since signals add directly, but noise only adds as power. The recent mechanically-coupled resonator array technique demonstrated in [6] might be ideal for this latter approach.

5. EXPERIMENTAL RESULTS

$2\mu\text{m}$ -thick, notched and un-notched (for comparative purposes), contour-mode hollow-disk ring resonators with 100 nm electrode-to-resonator gaps were fabricated via a three-polysilicon self-aligned-and-filled stem process used previously to achieve GHz frequency (but with lower Q) solid disk resonators [1]. Fig. 3 presents the SEM of a 1.2-GHz hollow-disk ring and a zoom-in on its central support, showing clearly the use of separate polysilicon depositions for the $2\mu\text{m}$ -thick ring suspension beams and the stem anchor filling. Fig. 4 presents the SEM of a notched version of this resonator made in the same fabrication process.

Despite their much-larger-than- 50Ω impedances, fabricated devices in the VHF range were still measurable in a direct two-port configuration via a network analyzer. At UHF, however, mismatch losses combine with parasitics to make two-port measurement difficult, so UHF devices were instead measured using a mixing technique [10], where the resonator bias voltage V_p is modulated to move motional currents away from parasitics, allowing for purer measurements via a spectrum analyzer. It should be noted that losses seen in the measured spectra to follow arise from impedance mismatching, and are not indicative of device loss. By their sheer high Q , it should be obvious that these devices will exhibit very little loss when used in properly matched filters [8].

Although recent work has shown that Q 's $>6,000$ in air are possible for UHF $\mu\text{mechanical}$ resonators [1], the devices of this work were measured in vacuum in order to isolate the anchor loss mechanisms that the subject suspension designs intend to alleviate. Fig. 5(a)-(b) present two-port-measured frequency characteristics for un-notched hollow-disk ring resonators vibrating in vacuum in the first contour-mode of Fig. 2(a), with bias voltages of 2.5 V and 7 V, center frequencies of 24.374 MHz and 72.07 MHz, and Q 's of 67,519 and 48,048, respectively. The extremely high Q of 67,519 at HF contributes to the very low series motional resistance of

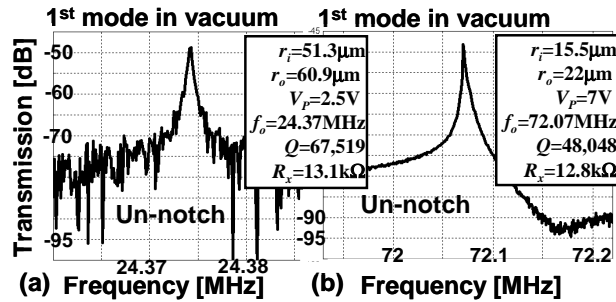


Fig. 5: Measured frequency characteristics for fabricated HF to VHF micromechanical hollow-disk ring resonators using a two-port measurement set-up under vacuum. (a) 1st mode 24.37MHz ring with direct support attachments, using a very small bias voltage of 2.5 V. (b) 1st mode 72.07MHz ring with direct support attachments, using a $V_p=7V$.

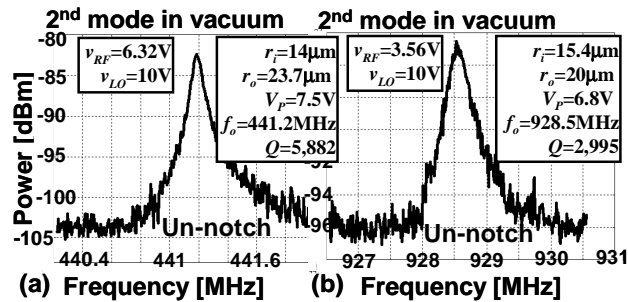


Fig. 6: Measured frequency characteristics for fabricated UHF micromechanical hollow-disk ring resonators using a mixing measurement set-up under vacuum. (a) 2nd mode 441.2MHz ring with direct support attachments. (b) 2nd mode 928.5MHz ring with direct support attachments.

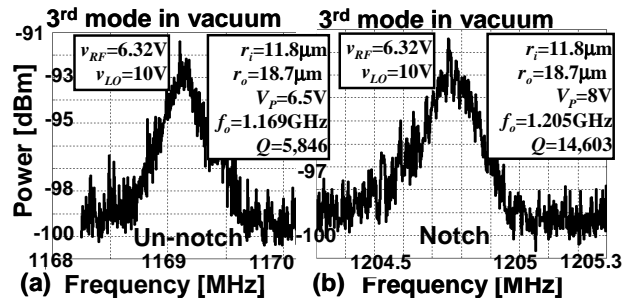


Fig. 7: Measured frequency characteristics for fabricated micromechanical hollow-disk ring resonators, all measured under vacuum using a mixing measurement set-up. (a) 3rd mode 1.169GHz ring with direct support attachments. (b) 3rd mode 1.205GHz ring with notched support attachments.

this resonator, which is only 13.1 k Ω with $V_p=2.5$ V. (A 10X higher bias voltage of 25 V, if permissible, would yield a 100X smaller R_x of 131 Ω .) Moreover, the average radius of the device measured in Fig. 5(a) is 3X larger than that of Fig. 5(b), which as predicted in Section 4, allows the former to achieve a similar R_x , despite the use of a smaller V_p .

Fig. 6(a)-(b) present frequency characteristics measured using the mixing method [10] for UHF hollow-disk rings vibrating in vacuum in the second (anti-symmetric) contour-mode of Fig. 2(b) and showing frequencies of 441.2 MHz and 928.5 MHz, with Q 's of 5,882 and 2,995, respectively. Fig. 7(a) presents the mixing-measured fre-

quency characteristic for an un-notched hollow disk ring resonator vibrating in vacuum in the third contour-mode with a center frequency of 1.169 GHz, and a Q of 5,846. Although already very good, this value of Q is more than doubled when ring notches are used to bring support attachments closer to true nodal locations. In particular, Fig. 7(b) finally presents the measured frequency characteristic for a third contour-mode hollow-disk ring resonator, now utilizing notches at the support attachment locations and showing a resonance frequency of 1.2048 GHz in vacuum with a Q of 14,603—a value now amenable to RF channel-select filters.

6. CONCLUSIONS

A “hollow-disk” ring resonator was described that used a centered, impedance-optimizing quarter-wavelength support structure with notched support-to-ring node attachments to achieve a record high Q of 14,603 at 1.2 GHz measured under vacuum. These values correspond to a frequency- Q product of 1.75×10^{13} , which is the highest yet seen for any polysilicon micromechanical resonator past 1 GHz, and which even exceeds the 1×10^{13} typically posted by some of the best quartz crystals. The sheer performance of this device might now bring the concept of RF channel-select filters for ultra-low-power wireless receivers much closer to reality, and in doing so, could revolutionize the design of wireless RF front-ends. From the results of this work, the minimization of anchor losses through anchor isolation is clearly among the most important design criteria when designing micromechanical resonators for frequencies past 1 GHz, and will likely continue to dominate among Q -limiting dissipation mechanisms as frequencies are pushed towards 10 GHz and beyond. Work towards such frequencies is ongoing.

Acknowledgment. This work was supported by DARPA and an NSF ERC on Wireless Integrated Microsystems.

References

- [1] J. Wang, *et al.*, "Self-aligned 1.14-GHz vibrating radial-mode disk resonators," *Transducers'03*, pp. 947-950.
- [2] B. Bircumshaw, *et al.*, "The radial bulk annular res.: towards a 50 Ω MEMS filter," *Transducers'03*, pp. 875-878.
- [3] M. A. Abdelmoneum, *et al.*, "Stemless wine-glass-mode disk umechanical resonators," *MEMS'03*, pp. 698-701.
- [4] J. Wang, *et al.*, "1.51-GHz nanocrystalline diamond micromechanical disk resonator with material-mismatched isolating support," *MEMS'04*, to be published.
- [5] J. R. Clark, *et al.*, "Parallel-resonator HF micromechanical bandpass filters," *Transducers'97*, pp. 1161-1164.
- [6] M. U. Demirci, *et al.*, "Mechanically corner-coupled square microresonator array for reduced series motional resistance," *Transducers'03*, pp. 955-958.
- [7] C. V. Stephenson, "Radial Vibrations in Short, Hollow Cylinders of Barium Titanate," *J. Acoust. Soc. Amer.*, Vol. 28, No. 1, 1956, pp. 51-56.
- [8] F. D. Bannon, *et al.*, "High- Q HF micromechanical filters," *IEEE J. Solid-State Circuits*, vol. 35, no. 4, pp. 512-526, April 2000.
- [9] R. Navid, *et al.*, "Third-order intermodulation distortion in capacitively-driven CC-beam micromechanical resonators," *MEMS'01*, pp. 228-231.
- [10] A.-C. Wong, *et al.*, "Micromechanical mixer+filters," *MEMS'98*, pp. 471-474.